Numerical framework of hybrid nanofluid over two horizontal parallel plates with non-linear thermal radiation

Umar Farooq [a], Hassan Waqas [b], Sobia Noreen [c], Muhammad Imran [a], Ali Akgül [d,e,f,*], Dumitru Baleanu [d,g,h], Sayed M.El Din [i], Taseer Muhammad [j], Ahmed M Galal [k,l]

[a] *Department of Mathematics, Government College University Faisalabad, 38000, Pakistan*
[b] *School of Energy and Power Engineering, Jiangsu University, Zhenjiang, 2122013, China*
[c] *Department of Chemistry, Government College Women University Faisalabad, 38000, Pakistan*
[d] *Department of Computer Science and Mathematics, Lebanese American University, Beirut, Lebanon*
[e] *Siirt University, Art and Science Faculty, Department of Mathematics, Siirt, 56100, Turkey*
[f] *Near East University, Mathematics Research Center, Department of Mathematics, Near East Boulevard, PC: 99138, Nicosia /Mersin 10-Turkey, Turkey*
[g] *Çankaya University, Department of Mathematics, Ankara Turkey*
[h] *Institute of Space Sciences, Magurele-Bucharest, R76900, Romania*
[i] *Center of Research, Faculty of Engineering, Future University in Egypt, New Cairo, 11835, Egypt*
[j] *Department of Mathematics, College of Sciences, King Khalid University, Abha, 61413, Saudi Arabia*
[k] *Department of Mechanical Engineering, College of Engineering in WadiAlddawasir, Prince Sattam bin Abdulaziz University, Saudi Arabia*
[l] *Production Engineering and Mechanical Design Department, Faculty of Engineering, Mansoura University, Mansoura, P.O 35516, Egypt*

ARTICLE INFO

ABSTRACT

Significance of study: High combustion temperatures necessitate appropriate cooling systems in the combustion process. Regenerative cooling is used in the majority of chambers in liquid propellant engines. The addition of nanoparticles to the cooling fluid is a novel technique to increase the efficiency of heat transfer in the regenerative cooling process.

Aim of the study: In this investigation, we investigate the two-dimensional flow of the hybrid nanofluid with suction/injection effect over two horizontal parallel plates. The non-linear thermal radiation effect is measured in the model of a hybrid nanofluid. Here we use single-walled carbon nanotubes, multi-walled carbon nanotubes, nickel-zinc iron oxide, and manganese zinc iron oxide with base fluid engine oil. The effects of different shape factors (Sphere, Bricks, Cylinder, Platelets, Column, and Lamina)are also incorporated.

Research methodology: Using appropriate similarity transformations, the controlling partial differential equations are transformed into ordinary differential equations. Using the shooting strategy, the transformed higher-order ordinary differential equations are converted to first-order ordinary differential equations, and the Bvp4c built-in function in MATLAB is used to produce the numerical and graphical results of the flow parameter.

Conclusion: The velocity profile is decreased by the increasing values of the suction/injection parameter. The temperature distribution profile declined for the higher values of the temperature ratio parameter. The combination of nickel zinc iron oxide and carbon nanotube nanomaterials to engine oil as a cooling fluid enhanced the heat transfer coefficient. According to the findings, carbon nanotubes outperform nickel zinc iron oxide nanoparticles in terms of increasing heat transfer coefficient and improving regenerative cooling.

1. Introduction

Nanofluids, as opposed to conventional fluids, perform a significant part in heat transmission improvement due to their high aspect ratio and thermal conductivity. The combination of tiny-sized solid fragments and base fluids can improve the temperature properties of several fluids. The nanoparticles of metals (e.g., Ag, Al, Cu, Si, Au, Ni, etc.) are frequently combined with metal oxide nanoparticles to create hybrid nanofluids. (i. e. ZnO, TiO3, WO3, ZrO2, CeO2, SnO2, etc.). When two different nanofluids are combined in a basic fluid, a homogeneous composition is formed. As a result, the produced compound has different physical and molecular properties. Ahmad et al. [1] studied the thermal features of a mixed nanofluid flow containing MnZnFe2O4, and NiZnFe2O4.

Nomenclature

$(u \& v)$	Components	(S)	Suction/injection parameter
$(B_1, B_2, B_3 \& B_4)$	Dimensionless constants	(θ)	Dimensionless temperature
(C_f)	Skin friction coefficients	(θ_w)	Temperature ratio parameter
$(f(\zeta))$	Similarity functions	(Ec)	Eckert number
(υ_{hnf})	Hybrid nanofluid kinematic viscosity	(Pr)	Prandtl number
(h)	Distance between the plates	$(\phi_1 = \phi_2)$	Nanoparticles volume fraction
(k_{hnf})	Hybrid nanofluid thermal conductivity	(ζ)	Dimensionless variable
(C_p)	Specific heat at constant pressure	(s)	Nano-solid-particles
(Nu)	Nusselt number	(μ_{hnf})	Hybrid nanofluid dynamic viscosity
(p)	Modified fluid pressure	(R)	Thermal radiation parameter
(hnf)	Hybrid nanofluid	(ρ_{hnf})	Hybrid fluid density
(α)	Viscosity parameter	(τ_w)	Skin friction or shear stress
		(f)	Base fluid

Muhammad and Nadeem [2] investigated the impacts of Ni-ZnFe2O4, Mn-ZnFe2O4, and Fe2O4 on ferromagnetic nanofluid material Zhao et al. [3] conducted a comparative investigation of ferromagnetic hybrid nanofluids under velocity slip and convective circumstances. Firew et al. [4] evaluated the efficiency and emissions of a CI engine running on ethanol diesel emulsified with a NiZnFe2O4 nanoparticle additive. The transfer of heat in MgZn_6Zr in Engine Oil was investigated by Noor and Mukhtar [5]. Maraj and Shaiq [6] investigated the rotational effect of tiny particles of Fe2O4, NiZnFe2O4, and MnZnFe2O4 in C2H6O2 contained between two stretchable discs. Barnoon [7] investigated the effects of heat transport and mixing quality in a microchannel fitted with a dual mixer. Kadhim et al. [8] examined the impact of hybrid nanofluid convective heat transfer in a porous container with wavy walls. Hirpho and Ibrahim [9] studied hybrid nanofluid convective heat transfer in a partially heated trapezoidal container. Salameh et al. [10] described nanofluid simulation and optimizing particle swarms. Ahmad et al. [11] used hybrid nanofluids to assess the endurance of a double-dimpled corrugated tube. The hydrothermal performance of a hybrid nanofluid was examined by Habeeb et al. [12]. Swamy et al. [13] examined the consequence of a magnetic field on the temperature distribution of an aqueous hybrid nanofluid flow between coaxial cylinders. Yahya and Saghir [14] studied the thermal effects of moving through a porous flat tube with a nanofluid. Çobanoğlu et al. [15] studied the flow characteristics of nanofluids based on an ethylene glycol mixture.

Hybrid nanofluids are a novel form of working fluid created by suspending two distinct kinds of nanoparticles with sizes (less than 100 nm) in a normal fluid. This novel type of nanofluid has greater thermal conductivity and thermophysical characteristics than traditional fluids. These hybrid nanofluids have recently been used in a variety of heat transmission uses such as heat pipe, solar power, cooling as well as heating, heater, airflow, conditioning system, coolant in machining and production, biomedical, space, spacecraft, military, and so on. Choi [16] coined the term nanostructures with the ultimate objective of increasing the thermophysical properties in mind. Buongiorno [17] developed a conceptual model for non-homogeneous equilibrium nanofluid mass transfer. Thermophoresis and Brownian motion are believed to be key slip tools in nanotechnology. Rashid et al. [18] examined the thermal conduction and von Kármán flow of nanofluid generated by an expanded plate. Das and Sarkar [19] put the fluid simulation results over two stretched spinning discs to the test. Sahoo and Shevchuk [20] investigated the characteristics of heat conductivity caused by the rotating flow of a fluid over a stretched sheet. Naqvi et al. [21] investigated the properties of a disk-generated nanofluid slip flow. Jaiswal [22] explored fluid past and distorted sphere motion. Shehzad et al. [23] used the CattaneoChristov and bioconvection theories to study the impact of Maxwell nanoparticles on a single disk.

When a more comprehensive form of the radiation effect for a fluid flow issue is needed, the nonlinear mathematical representation of thermal radiation is used. Thermal radiations have many applications in science and technology and material research, including glass production, material production, thermonuclear reactor cooling fluid, and furnace design. In addition, thermal radiations have beneficial uses in space transformation genetic factors like rockets; rocket streamlines characteristics, propellant system, and spaceship operating system at greater temperatures. Many studies [28–30] have been performed because of its important uses, with the main emphasis on the utilization of thermal radiations by utilizing the linear form of Roseland flow. Ferdows et al. [24] studied the effect of two-dimensional microbes on the transport of MHD nanomaterials across extended surfaces. Gangadhar et al. [25] examined the features of discontinuous free variable flow nanofluid flow on a stretched surface using a spectrum coping approach. Jawad et al. [26] studied the influence of thermal radiation and impairment on entropy formation and heat transmission in a nanostructure aqueous solution in an unstable spinning MHD. Ali et al. [27] studied the fundamental properties of a magnetic flow combustion method. Nisar et al. [28] studied the influence of activation energy in nanoparticle photonic peristaltic flow. Muhammad et al. [29] investigated the effect of melting temperature variations on the movement of conventional fluids, CNTs, and hybrid nanofluid water. Waqas et al. [30] looked at the two-dimensional flow patterns of intriguing hybrid nanofluids during heat transfer. Waqas et al. [31] studied the MHD flow of a hybrid nanofluid flow across a disk. Waqas et al. [32] investigated surface-catalyzed reactions in a nanofluid flow. Muhammad et al. [33] used infrared light to investigate the influence of melting thermal performance in nanofluid flow over a sheet. Fadaei et al. [34] looked at the effects of non-Newtonian phase transitions in a shell-and-tube heat exchanger. Izadi et al. [35] investigated how the cooling process affects thermal energy storage. Izadi et al. [36] examined the use of a fin in an H-shaped heat recovery device for charging phase change material. Izadi et al. [37] statistically examined the annular Al2O3/water nanofluid laminar convection flow. Izadi et al. [38] explored the engine cooling of a nanofluid flow in a heat sink circular tube with an axial conductivity effect. The time-dependent flow of a nanofluid across a shrinking/stretching surface was investigated by Lanjwani et al. [39]. Xiong et al. [40] looked at a variety of hybrid nanofluid uses in solar energy collectors. The role of carbon-based nanofluids in various heat exchangers was the subject of this review research. This is because graphene and carbon nanotubes have better thermophysical characteristics than other nanostructures [41]. In comparison to other nanoparticles, graphene, and carbon nanotubes offer extremely high heat transfer [42], lower population density [43], a massive anamorphic widescreen [44], higher stability [45], less degradation and corrosion [46], and lower pressure drop [47] and flow rates [48]. Hybrid propellants are environmentally friendly and have a high specific impulse that is between liquid and solid propellants [49–50].

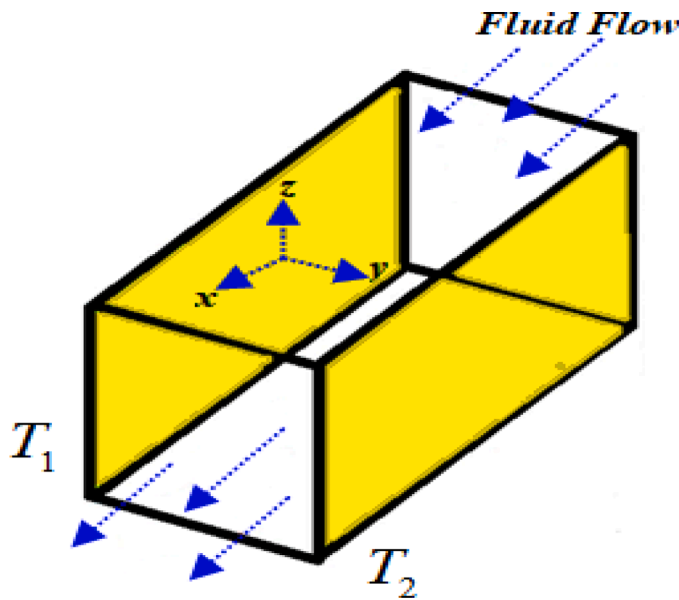The scope of the current framework is to analyze the importance of a
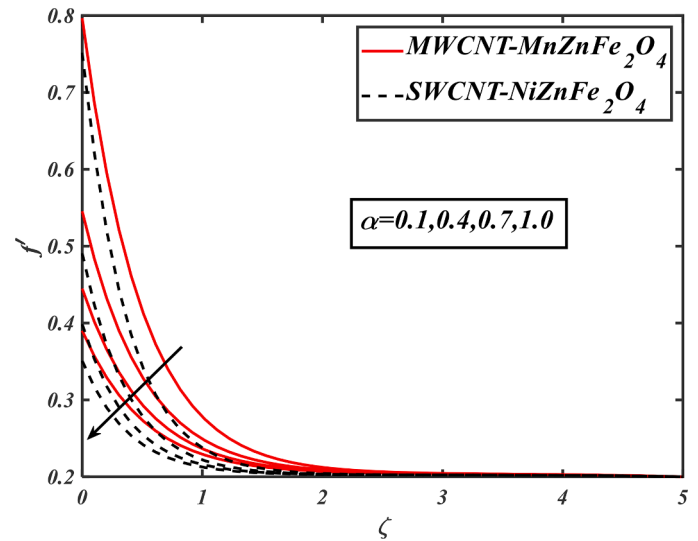
Fig. 1. Physical descriptions of the problem.

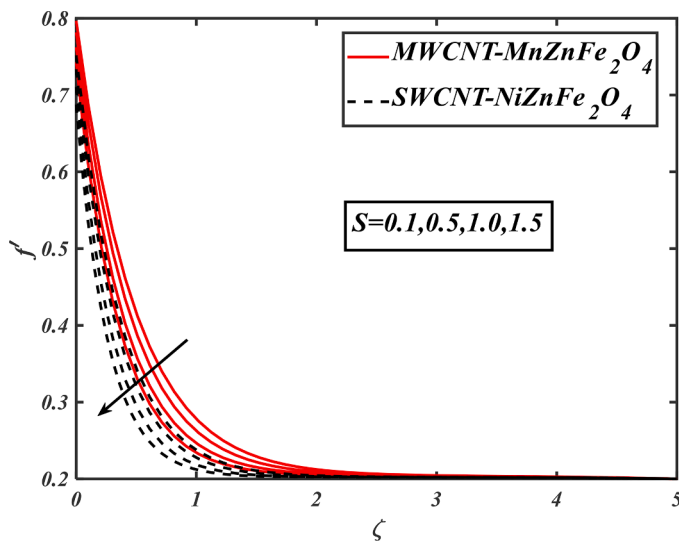

Fig. 3. Aspect of α over f'.

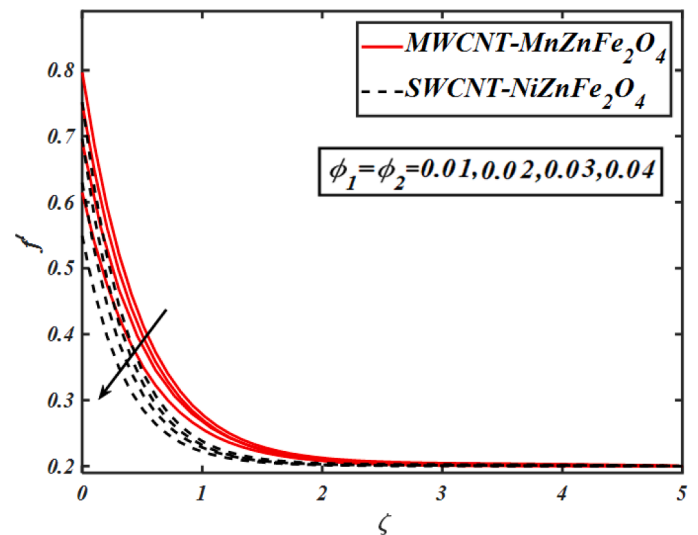**Fig. 2.** Aspect of S over f'.

Fig. 4. Aspect of $\phi_1 = \phi_2$ over f'.

hybrid nanofluid with non-linear thermal radiation and section/injection effects passing through two horizontal parallel plates. Physically this problem examines the heat transfer improvement inside two horizontal parallel plates with engine oil-based nanofluid containing nanoparticles including carbon nanotube, nickel-zinc iron oxide($NiZnFe_2O_4$), and manganese zinc iron oxide ($MnZnFe_2O_4$) with base fluid engine oil. The current issue is mathematically designed in the form of nonlinear PDEs with relative boundary constraints and then converted into proper dimensionless forms by using similarity transformations. The dimensionless coupled equations are integrated utilizing the shooting algorithm over the bvp4c package in MATLAB. The effects of different value flow parameters on subjective flow profiles are discussed and elaborated through graphs. Some examples of hybrid nanofluid uses include heat pumps and heating elements, coolants in machining and production, generator cooling, heating, ventilation, refrigeration, solar collectors, and conditioning systems applications.

2. Physical description and modeling

2.1. Physical description

The steady flow of hybrid nanofluid with heat transfer over two horizontal plates is investigated in this work (see Fig. 1). The source is placed on the bottom plate, and the plates are at $y = 0$ and $y = h$. Two equal and opposing pressures stretch the bottom plate, resulting in the point (0; 0; 0) remaining in the same position. Here engine oil base fluid ($MWCNT - MnZnFe_2O_4$)and($SWCNT - NiZnFe_2O_4$) nanoparticles are used. The hybrid nanofluid is a more than two-particle mixture with assumptions as follows:

- Two-dimensional steady flow
- Thermal radiation effects
- Two horizontal plates geometry
- To investigate the heat transfer in the nozzle of the rocket we use Engine oil-based nanofluid having nanoparticles
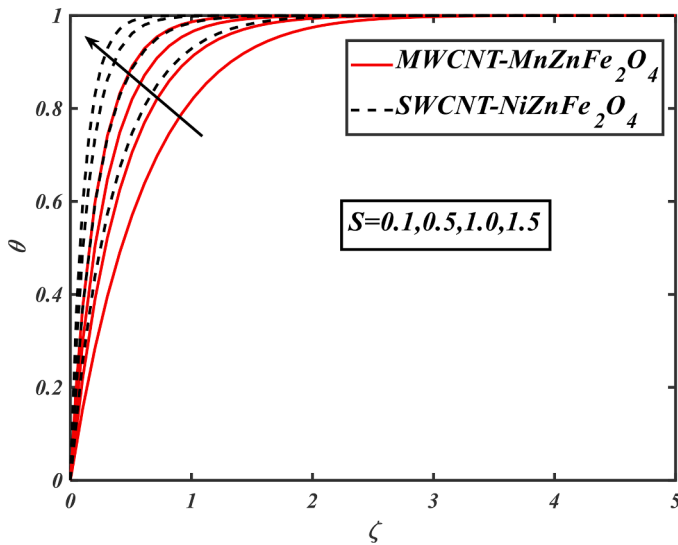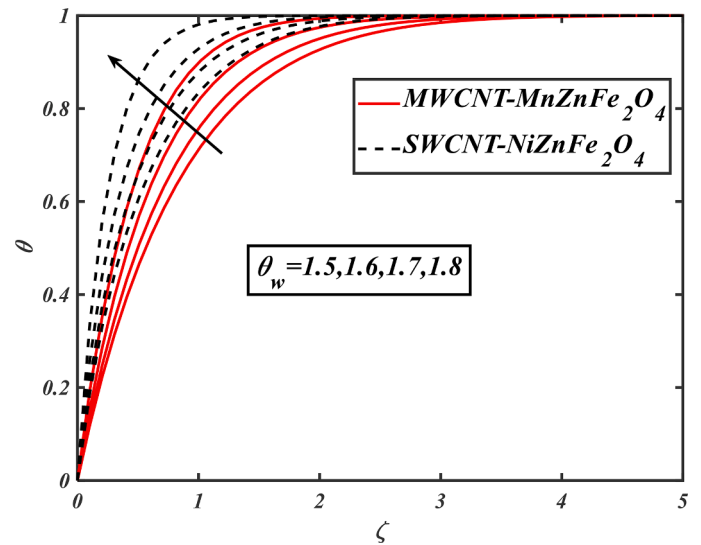
Fig. 5. Aspect of S over θ.

Fig. 7. Aspect of θ_w over θ.

Boltzmann constant and $(T = T_\infty[1 + (\theta_w - 1)])$ with temperature ratio $\left(\theta_w = \frac{T_w}{T_\infty}\right)$

2.3. Boundary constraints

The boundary conditions are [51–52].

$$\left.\begin{array}{l} u = bx, v = 0, T = T_h \ \ at \ y = 0 \\ u = 0, v = 0, \ \ T = T_0 \ \ at \ \ y = h \end{array}\right\}, \tag{6}$$

2.4. Thermophysical properties

The density of hybrid nanofluid(ρ_{hnf}), the heat capacity of hybrid nanofluid((ρC_p)$_{hnf}$), (μ_{hnf})the dynamic viscosity of hybrid nanofluid, and the thermal conductivity of hybrid nanofluid (k_{hnf}), are defined as:

$$\left.\begin{array}{l} \rho_{hnf} = (1 - \Phi)\rho_f + \Phi\rho_s, \mu_{hnf} = \dfrac{\mu_f}{(1 - \Phi)^{2.5}}, \\[2mm] \left(\rho C_p\right)_{hnf} = (1 - \Phi)\left(\rho C_p\right)_f + \Phi\left(\rho C_p\right)_s, \\[2mm] \dfrac{k_{hnf}}{k_f} = \dfrac{k_s + 2k_f - 2\Phi\left(k_f - k_s\right)}{k_s + 2k_f + 2\Phi\left(k_f - k_s\right)} \end{array}\right\}, \tag{7}$$

2.5. Similarity transformations

The suitable similarity transformations are [51–52].

$$u = axf^{'}(\zeta), v = ahf(\zeta), \ \zeta = \frac{y}{h}, \theta(\zeta) = \frac{T - T_0}{T_h - T_0}\bigg\}, \tag{8}$$

2.6. Dimensional form governing equations

As a result, the dimensionless velocity and heat equations for this problem are as follows:

$$f'''' - \alpha\frac{B_1}{B_2}\left(f^{'}f^{''} - ff^{'''}\right) = 0, \tag{9}$$
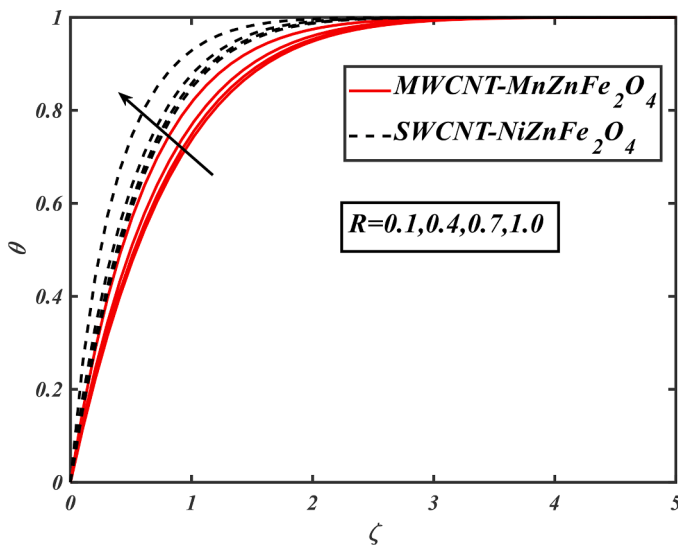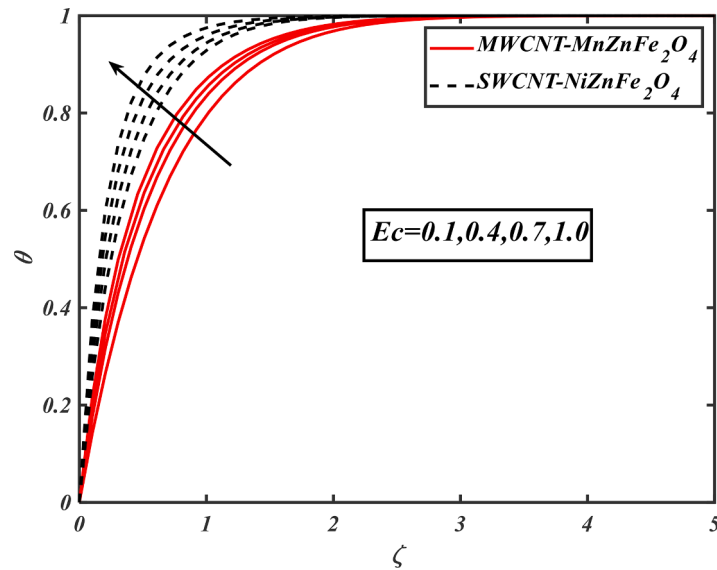

Fig. 6. Aspect of R over θ.

2.2. Mathematical modeling

The main equations (equation of continuity, momentum equation, and thermal equations) are written as [51–52]:

$$u_x + v_y = 0, \tag{1}$$

$$\rho_{hnf}\left(uu_x + vu_y\right) = -p_x^* + \mu_{hnf}\left(u_{xx} + u_{yy}\right), \tag{2}$$

$$\rho_{hnf}\left(uv_x + vv_y\right) = -p_y^* + \mu_{hnf}\left(v_{xx} + v_{yy}\right), \tag{3}$$

$$\left(\rho C_p\right)_{hnf}\left(uT_x + vT_y\right) = k_{hnf}\left(T_{xx} + T_{yy}\right) + \mu_{hnf}\left(2\left[\left(u_x\right)^2 + \left(v_y\right)^2\right] + \left(v_x\right)^2\right)$$
$$- \left(q_r\right)_y, \tag{4}$$

Where($u\&v$)shows the components in the ($x\&y$) directions, (T) is temperature, (p) is the modified fluid pressure.

$$q_r = \frac{-4\sigma^*}{3k^*}T_y^4 = \frac{-16\sigma^*}{3k^*}T_\infty^3 T_y \tag{5}$$

Where(k^*)and (σ^*)are mean absorption coefficient and Stefan
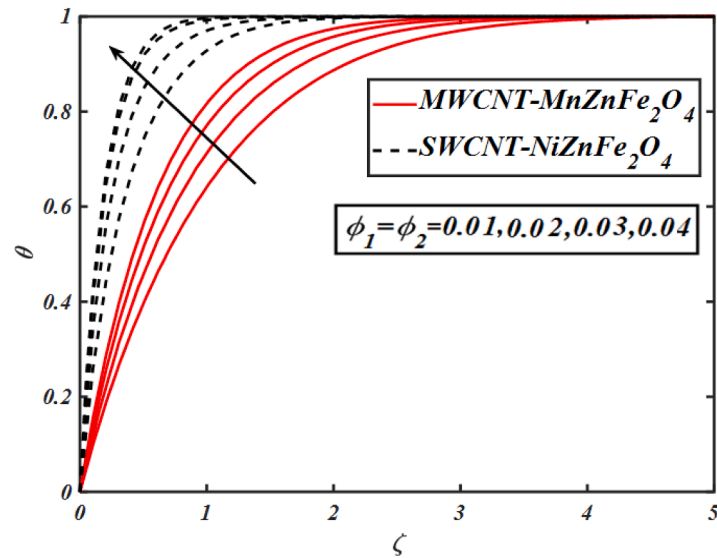
Fig. 8. Aspect of Ec over θ.

Fig. 9. Aspect of $\phi_1 = \phi_2$ over θ.

$$\left[\frac{1}{\Pr}\frac{k_{hnf}}{k_f} + R(1 + (\theta_w - 1)\theta)^3\right]\theta'' + \left[\frac{4R}{\frac{k_{hnf}}{k_f}}(1 + (\theta_w - 1)\theta)^2(\theta_w - 1)\right]\theta'^2$$

$$+\Pr\frac{B_2 B_3}{B_1 B_4}\left[R\frac{B_1}{B_2}f\theta' + Ec\frac{B_1}{B_3}\left(4f'^2\right)\right] = 0, \tag{10}$$

With

$$\left.\begin{array}{l} f = S, f' = 1, \theta = 1 \ at \ \zeta = 0 \\ f = 0, f' = 0, \theta = 1 \ at \ \zeta = \infty \end{array}\right\}, \tag{11}$$

$$\alpha\left(=\frac{ah^2}{v_f}\right), Pr\left(=\frac{\mu_f(\rho C_p)_f}{\rho_f k_f}\right), Ec\left(=\frac{\rho_f a^2 h^2}{(\rho C_p)_f(\theta_0 - \theta_h)}\right), \theta_w\left(=\frac{T_w}{T_\infty}\right)\right\}, \tag{12}$$

Here (α)is the viscosity parameter, (θ_w) temperature ratio parameter, (S) suction/injection parameter, (Pr)Prandtl number, and (Ec) Eckert number,

2.7. Physical quantities of major interest

The skin fraction is defined as:

$$C_f = \left[\frac{B_2}{B_1}f''(0)\right]. \tag{13}$$

The Nusselt number is given as:

$$Nu = \left[\left(\frac{k_{hnf}}{k_f}\right)\theta'(0)\right]. \tag{14}$$

3. Numerical procedure

In this portion, the velocity and temperature nonlinearly ordinary differential equations (09-10) with associated reduced boundary constraints (11) are numerically tackled by adopting the shooting scheme over bvp4c solver in computational MATLAB which is dependent on the
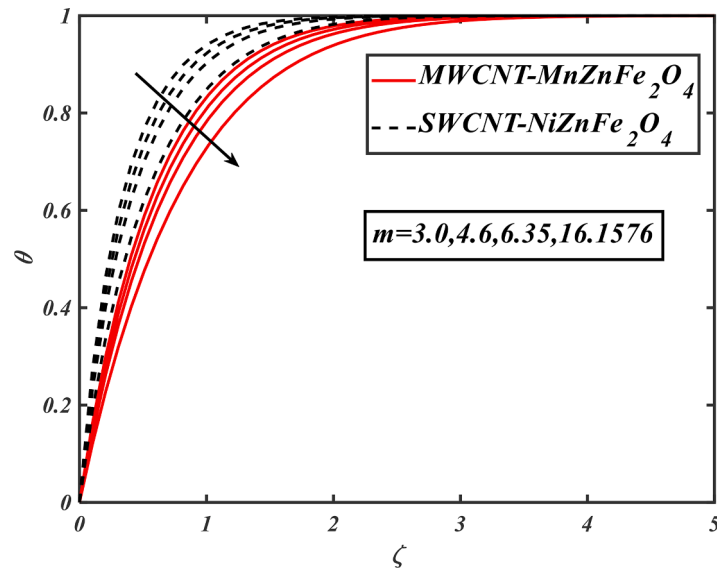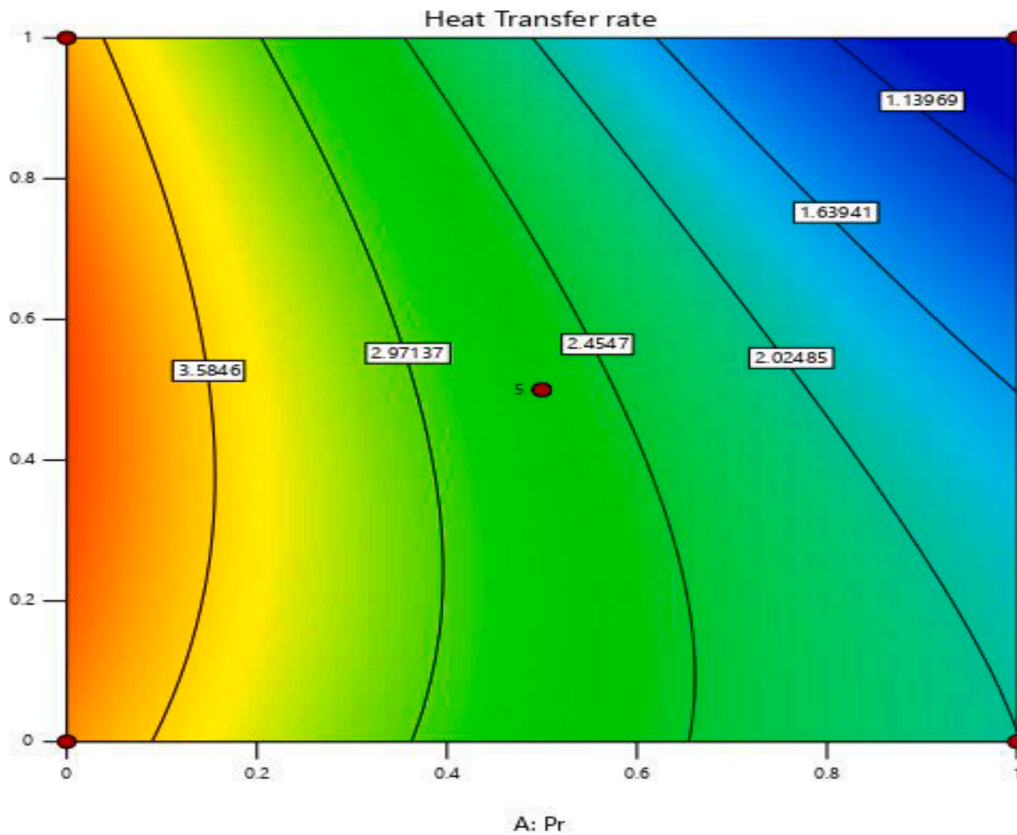
Fig. 10. Aspect of m over θ.

Fig. 11. Contour plot of Pr&Ec.

three stages Lobatto formula for different involving prominent parameters. The Lobatto-IIIa method is a collection phenomenon under the fourth-order accuracy. Firstly, for this procedure, the higher-order ordinary differential equations are converted into ordinary ones with the help of new considerations. All the numerical significances exemplified in this problem are pondered to an error of tolerance 10^{-6}.

Let

$$\left.\begin{array}{lll} f = p_1, & f' = p_2, & f'' = p_3, \\ f''' = p_4, & & f'''' = p'_4, \\ \theta = p_5, & \theta' = p_6, & \theta'' = p'_6 \end{array}\right\}, \tag{15}$$

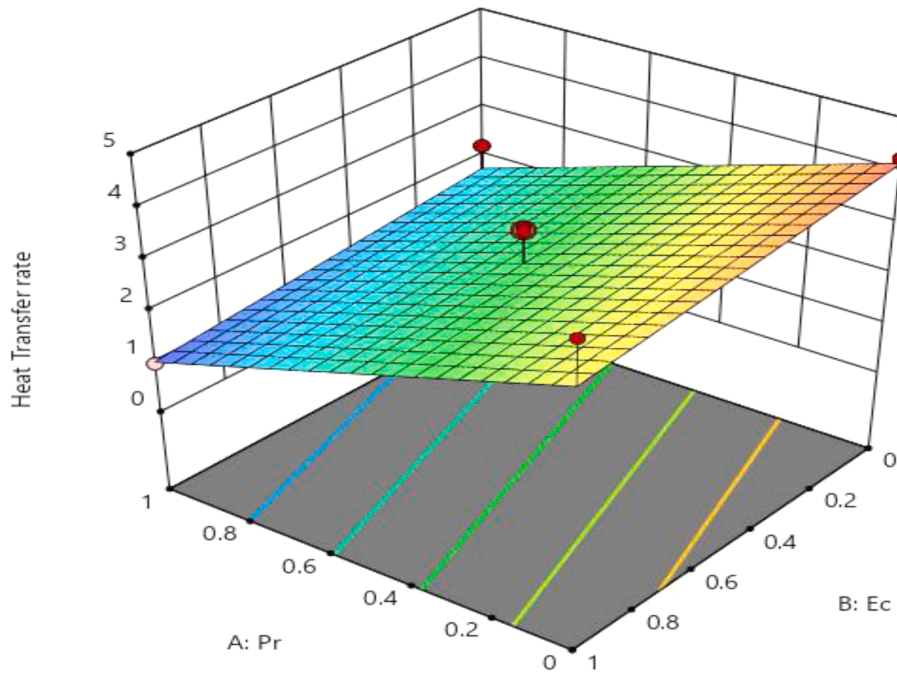$$p'_4 = \alpha\frac{B_1}{B_2}(p_2p_3 - p_1p_4), \tag{16}$$
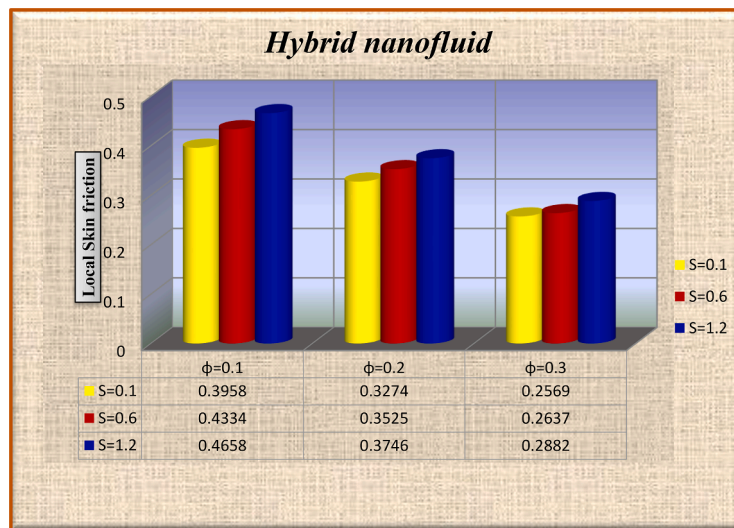
Fig. 12. 3D surface plot of Pr&*Ec*.

Fig. 13. Bar chart for local skin friction number.

$$p_6' = \frac{-\Pr\frac{B_2 B_3}{B_1 B_4}\left[R\frac{B_1}{B_2}p_1 p_6 + Ec\frac{B_1}{B_3}\left(4p_2{}^2\right)\right]}{\left[\frac{1}{\Pr}\frac{k_{hnf}}{k_f} + R(1 + (\theta_w - 1))\right]}, \tag{17}$$

With

$$\left.\begin{array}{l} p_1 = S, p_2 = 1, p_5 = 1 \\ at\ \zeta = 0 \\ p_1 = 0, p_2 = 0, p_5 = 1 \\ at\ \zeta = \infty \end{array}\right\}, \tag{18}$$

4. Results and discussions

The major role of this section is to perceptibly elucidate the physical significance of the graphical consequences. The graphs are used to examine fluctuations in velocity and temperature profiles instigated by increasing and decreasing variations of physical parameters. To inves-tigate the nature of the velocity profile Figs. 2-14 are stretched. Fig. 2 shows the performance of the suction/injection parameter(*S*)on the velocity field (*f′*). The velocity filed (*f′*)decreased for the enhancement in the variations of suction/injection parameter (*S*)for both hybrid nano-fluids.Suction/injection is a mechanical process that is employed to decrease energy losses in the boundary layer area by lowering surface drag. The red solid line shows the behavior of ($MWCNT - MnZnFe_2O_4$) and the black dish line performs($SWCNT - NiZnFe_2O_4$)with base fluid engine oil. The characteristic of the viscosity parameter (α)on the ve-locity profile (*f′*)is plated in Fig. 3. The velocity distribution profile(*f′*) diminishes for the higher estimations of the viscosity parameter (α) and the red solid line shows the behavior of ($MWCNT - MnZnFe_2O_4$)and the black dish line performs($SWCNT - NiZnFe_2O_4$)with base fluid engine oil. The consequence of (φ₁ = φ₂)the velocity distribution profile (*f′*)is depicted in Fig. 4. It is found that the augmentation of the estimations (φ₁ = φ₂) decreased(*f′*). It has been shown that bigger changes in solid

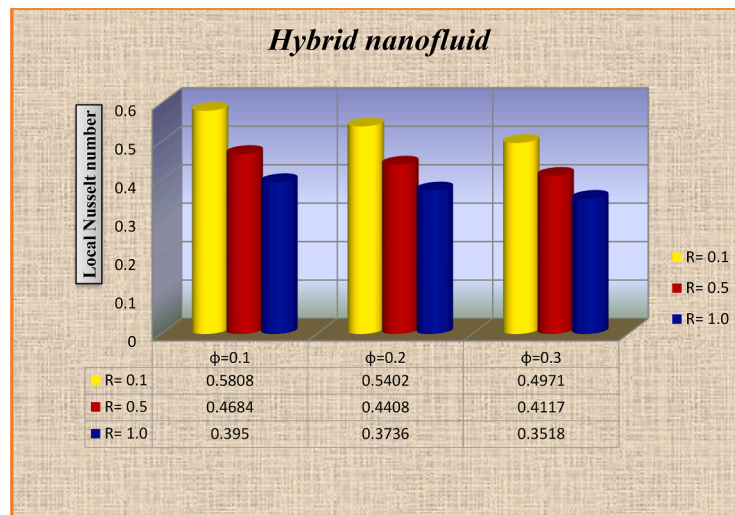**Fig. 14.** Bar chart for local Nusselt number.

The bar chart data:

	$\phi=0.1$	$\phi=0.2$	$\phi=0.3$
R= 0.1	0.5808	0.5402	0.4971
R= 0.5	0.4684	0.4408	0.4117
R= 1.0	0.395	0.3736	0.3518

Table 1

Thermophysical values of nanoparticles [53–54].
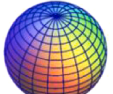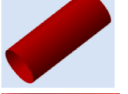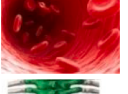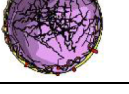
Thermophysical Properties	ρ (kg/m^3)	C_p (J/kgK)	k (W/mK)
Single-walled carbon nanotube	2600	425	6600
(SWCNT)			
Multi-walled carbon nanotube	1600	796	300
(MWCNT)			
Nickel zinc iron oxide	4800	710	6.3
($NiZnFe_2O_4$)			
Manganese zinc iron oxide	4700	1050	3.9
($MnZnFe_2O_4$)			
Engine oil	884	1910	0.144
(EO)			

Table 2

The geometrical appearance of nanoparticles and shape factor [55–56].

Geometry	Shape	Shape Factor
	3.0	Sphere
	3.7	Bricks
	4.9	Cylinders
	5.7	Platelets
	6.3598	Column
	16.1576	Lamina

volume friction enhance the velocity of the fluid element. The influences of suction/injection parameter(S) on a temperature distribution profile $(\theta)$for both cases and the red solid line show the behavior of $(MWCNT - MnZnFe_2O_4)$and the red dish line performs$(SWCNT - NiZnFe_2O_4)$with base fluid engine oil are illustrated in Fig. 5. It is scrutinized that the rising values of the suction/injection parameter(S)enhance the temperature profile(θ). The aspect of the (R) on (θ) is plotted in Fig. 6. The

heat distribution profile is raised by growing values of the thermal radiation parameter(R). The red solid line shows the behavior of $(MWCNT - MnZnFe_2O_4)$and the black dish line performs$(SWCNT - NiZnFe_2O_4)$ with base fluid engine oil. The impact temperature ratio parameter(θ_w) $(\theta)$is shown in Fig. 7.The (θ)increase for higher values of temperature ratio parameter(θ_w). The red solid line shows the behavior of $(MWCNT - MnZnFe_2O_4)$and the black dish line performs$(SWCNT - NiZnFe_2O_4)$ with base fluid engine oil. The aspects of (Ec) on temperature distribution profile$(\theta)$are shown in Fig. 8. The heat filed(θ)increased by the increasing estimations of the Eckert number(Ec). The Eckert number is employed to describe the significance of dissipation effects on the self-heating of a fluid. Fig. 9 displays the aspects of $(\phi_1 = \phi_2)$the temperature distribution profile(θ). The thermal field$(\theta)$is boosted up for the increasing values of nanoparticles volume fraction$(\phi_1 = \phi_2)$. The aspect of the shape factor of nanoparticles (m)on the temperature distribution profile$(\theta)$is shown in Fig. 10. When the values of the shape factor (m)

Table 3

Comparison of the shooting technique and the numerical approach for the velocity and temperature profiles.

(ζ)	Acharya et al. [57] Velocity profile Shooting method	Numerical	Temperature profile Shooting method	Numerical	Current Work Velocity profile Shooting method	Numerical	Temperature profile Shooting method	Numerical
0.0	0.0	0.0	0.0	0.0	1.0	1.0	1.0	1.0
0.1	0.080674	0.080670	0.080674	0.080670	0.860820	0.860817	0.860820	0.860817
0.2	0.127050	0.127048	0.127050	0.127048	0.725141	0.725138	0.725141	0.725138
0.3	0.145489	0.145482	0.145489	0.145482	0.602247	0.602246	0.602247	0.602246
0.4	0.142158	0.142153	0.142158	0.142153	0.494065	0.494063	0.494065	0.494063
0.5	0.123119	0.123112	0.123119	0.123112	0.398511	0.398507	0.398511	0.398507
0.6	0.094351	0.094346	0.094351	0.094346	0.312051	0.312048	0.312051	0.312048
0.7	0.061792	0.061786	0.061792	0.061786	0.231230	0.231226	0.231230	0.231226
0.8	0.031330	0.031323	0.031330	0.031323	0.153317	0.153314	0.153317	0.153314
0.9	0.008794	0.008793	0.008794	0.008793	0.076526	0.076524	0.076526	0.076524
1.0	0.0	0.0	0.0	0.0	0.0	0.0	0.0	0.0

increased the temperature profile(θ)decreased.Figure: 12and 13display the contour and 3D plot of both flow parameters like the Prandtl number(Pr)(Ec). Figures: 14 and 15 show the statistical analysis for the Local Skin Resistance Number and Local Nusselt Number for flow parameters and in both cases, the red solid line shows the behavior of ($MWCNT - MnZnFe_2O_4$) the black dish line performed($SWCNT - NiZnFe_2O_4$)with base fluid machine oil. Table 1 shows the thermophysical properties of nanoparticles (($SWCNT$),($MWCNT$)),($NiZnFe_2O_4$) and ($MnZnFe_2O_4$)with base fluid engine oil(EO). Table 2 analyzes the shape factors of Sphere (3.0), Bricks (3.7), Cylinders (4.9), Platelets (5.7), Columns (6.3598), and Lamina (16.1576). Table 3 displays the comparison of the shooting technique and the numerical approach for the velocity and temperature profiles. It shows the good agreement between published and current work.

5. Concluding remarks

The influence of hybrid nanofluid flow with non-linear thermal radiation and nanoparticles like carbon nanotube (($SWCNT$),($MWCNT$)), nickel-zinc iron oxide ($NiZnFe_2O_4$)and manganese zinc iron oxide ($MnZnFe_2O_4$)with base fluid engine oil(EO)in a liquid rocket engine nozzle is investigated in the current article. The main partial differential equations are converted into ordinary differential equations by using similarities transformations. The Bvp4c solver is used in the computational software MATLAB to compute the graphical outcomes of the flow parameters.

Some key concluding remarks are as follows:

- The augmentation in the intensity of the suction/injection parameter (S)and viscosity parameter (α)diminutions the velocity profile
- The enchantment in the values of the volume fraction of nanoparticles ($\phi_1 = \phi_{12}$)decline the velocity profile while boosted up the (θ)
- The augmentation in the estimations of suction/injection parameter (S) and Eckert number(Ec) increases the temperature contour
- The temperature profile is boomed for the higher values of temperature ratio parameter(θ_w) while decays for the greater variations of shape factor parameter(m)

Declaration of Competing Interest

The authors state that they have no known conflicting financial interests or personal ties that would appear to impugn the work described in this study.

Data availability

The data that has been used is confidential.

References

[1] S. Ahmad, S. Akhter, M.I. Shahid, K. Ali, M. Akhtar, M. Ashraf, Novel thermal aspects of hybrid nanofluid flow comprising of manganese zinc ferrite MnZnFe2O4, nickel-zinc ferrite NiZnFe2O4, and motile microorganisms, Ain Shams Eng. J. 13 (5) (2022), 101668.

[2] N. Muhammad, S. Nadeem, Ferrite nanoparticles Ni-ZnFe 2 O 4, Mn-ZnFe 2 O 4, and Fe 2 O 4 in the flow of ferromagnetic nanofluid, The Eur. Phys. J. Plus 132 (2017) 1–12.

[3] T.H. Zhao, M.I. Khan, S. Qayyum, R.N. Kumar, Y.M. Chu, B.C. Prasannakumara, Comparative study of ferromagnetic hybrid (manganese zinc ferrite, nickel zinc ferrite) nanofluids with velocity slip and convective conditions, Physica Scripta 96 (7) (2021), 075203.

[4] D. Firew, R.B. Nallamothu, G. Alemayehu, R. Gopal, Performance and emission evaluation of CI engine fueled with ethanol diesel emulsion using NiZnFe2O4 nanoparticle additive, Heliyon 8 (11) (2022) e11639.

[5] S. Noor, S. Mukhtar, Study of heat transfer in magnesium zinc zirconium MgZn_6Zr alloy suspended in engine oil, J. Math. 2021 (2021) 1–8.

[6] E.N. Maraj, S. Shaiq, Rotational impact on nanoscale particles Fe2O4, NiZnFe2O4, MnZnFe2O4 suspended in C2H6O2 confined between two stretchable disks: a computational study, Can. J. Phys. 98 (3) (2020) 312–325.

[7] P. Barnoon, Numerical assessment of heat transfer and mixing quality of a hybrid nanofluid in a microchannel equipped with a dual mixer, Int. J. Thermofluids 12 (2021), 100111.

[8] H.T. Kadhim, A. Al-Manea, A.N. Al-Shamani, T &Yusaf, Numerical analysis of hybrid nanofluid natural convection in a wavy walled porous enclosure: local thermal non-equilibrium model, Int. J. Thermofluids 15 (2022), 100190.

[9] M. Hirpho, W. Ibrahim, Modeling and simulation of hybrid Casson nanofluid mixed convection in a partly heated trapezoidal enclosure, Int. J. Thermofluids 15 (2022), 100166.

[10] T. Salameh, P.P. Kumar, E.T. Sayed, M.A. Abdelkareem, H. Rezk, A.G &Olabi, Fuzzy modeling and particle swarm optimization of Al2O3/SiO2 nanofluid, Int. J. Thermofluids 10 (2021), 100084.

[11] F. Ahmad, S. Mahmud, M.M. Ehsan, M &Salehin, Thermo-hydrodynamic performance evaluation of double-dimpled corrugated tube using single and hybrid nanofluids, Int. J. Thermofluids (2023), 100283.

[12] A.S. Habeeb, S. Aljabair, A.A &Karamallah, Experimental and numerical assessment on hydrothermal behavior of MgO-Fe3O4/H2O hybrid nano-fluid, Int. J. Thermofluids 16 (2022), 100231.

[13] H.K. Swamy, N.K. Reddy, M. Sankar, P.R &Peddinti, Conjugate heat transfer of aqueous hybrid nano liquid between coaxial cylinders subjected to the magnetic field, Int. J. Thermofluids 17 (2023), 100299.

[14] M. Yahya, M.Z &Saghir, Thermal analysis of flow in a porous flat tube in the presence of a nanofluid: numerical approach, Int. J. Thermofluids 10 (2021), 100095.

[15] N. Çobanoğlu, A. Banisharif, P. Estellé, Z.H &Karadeniz, The developing flow characteristics of water-ethylene glycol mixture based Fe3O4 nanofluids in eccentric annular ducts in low-temperature applications, Int. J. Thermofluids 14 (2022), 100149.

[16] S.U.S. Choi, J. Eastman, Enhancing thermal conductivity of fluids with nanoparticles, ASME-Publications-Fed. 231 (6) (2001) 718–720.

[17] Buongiorno, Convective transport in nanofluids, J. Heat Transf. 128 (3) (2006) 240–250.

[18] M.U. Rashid, M. Mustafa, A study of heat transfer and entropy generation in von Kármán flow of Reiner-Rivlin fluid due to a stretchable disk, Ain Shams Eng. J. (2020).

[19] A. Das, S &Sarkar, Flow analysis of Reiner–Rivlin fluid between two stretchable rotating disks. Recent Trends in Wave Mechanics and Vibrations, Springer, Singapore, 2020, pp. 61–70.

[20] B. Sahoo, I.V &Shevchuk, Heat transfer due to the revolving flow of Reiner-Rivlin fluid over a stretchable surface, Therm. Sci. Eng. Progress 10 (2019) 327–336.

[21] S.M.R.S. Naqvi, H.M. Kim, T. Muhammad, F. Mallawi, M.Z &Ullah, Numerical study for slip flow of Reiner-Rivlin nanofluid due to a rotating disk, Int. Commun. Heat and Mass Transf. 116 (2020), 104643.

[22] B.R. Jaiswal, Stokes flow of reiner-rivlin fluid past a deformed sphere, Int. J. Fluid Mech. Res. 46 (5) (2019).

[23] S.A. Shehzad, M.G. Reddy, A. Rauf, Z. Abbas, Bioconvection of Maxwell nanofluid under the influence of double-diffusive Cattaneo–Christov theories over an isolated rotating disk, Physica Scripta 95 (4) (2020), 045207.

[24] M. Ferdows, M.G. Reddy, S. Sun, F &Alzahrani, Two-dimensional gyrotactic microorganisms flow of hydromagnetic power-law nanofluid past an elongated sheet, Adv. Mech. Eng. 11 (11) (2019), 1687814019881252.

[25] K. Gangadhar, T. Kannan, G. Sakthivel, K &DasaradhaRamaiah, Unsteady free convective boundary layer flow of a nanofluid past a stretching surface using a spectral relaxation method, Int. J. Ambient Energy 41 (6) (2020) 609–616.

[26] M. Jawad, Z. Shah, A. Khan, W. Khan, P. Kumam, S. Islam, Entropy generation and heat transfer analysis in MHD unsteady rotating flow for aqueous suspensions of carbon nanotubes with nonlinear thermal radiation and viscous dissipation effect, Entropy 21 (5) (2019) 492.

[27] M. Ali, F. Sultan, W.A. Khan, M. Shahzad, H &Arif, Important features of expanding/contracting cylinder for Cross magneto-nanofluid flow, Chaos, Solitons& Fractals 133 (2020), 109656.

[28] Z. Nisar, T. Hayat, A. Alsaedi, B. Ahmad, Significance of activation energy in radiative peristaltic transport of Eyring-Powell nanofluid, Int. Commun. Heat and Mass Transf. 116 (2020), 104655.

[29] K. Muhammad, T. Hayat, A. Alsaedi, B. Ahmad, Melting heat transfer in squeezing flow of base fluid (water), nanofluid (CNTs+ water), and hybrid nanofluid (CNTs+ CuO+ water), J. Therm. Anal. Calorim. (2020) 1–18.

[30] H. Waqas, U. Farooq, M. Alghamdi, T. Muhammad, A.S &Alshomrani, On the magnetized 3D flow of hybrid nanofluids utilizing nonlinear radiative heat transfer, Physica Scripta (2021).

[31] H. Waqas, U. Farooq, R. Naseem, S. Hussain, M &Alghamdi, Impact of MHD radiative flow of hybrid nanofluid over a rotating disk, Case Stud. Therm. Eng. (2021) 101015.

[32] H. Waqas, U. Farooq, M. Alghamdi, T. Muhammad, Significance of surface-catalyzed reactions in SiO2-H2O nanofluid flow through porous media, Case Stud. Therm. Eng. (2021) 101228.

[33] T. Muhammad, H. Waqas, U. Farooq, M.S &Alqarni, Numerical simulation for melting heat transport in nanofluids due to quadratic stretching plate with nonlinear thermal radiation, Case Stud. Therm. Eng. (2021) 101300.

[34] M. Fadaei, M. Izadi, E. Assareh, A &Ershadi, Conjugated non-Newtonian phase change process in a shell and tube heat exchanger: a parametric-geometric analysis, Appl. Therm. Eng. 220 (2023), 119795.

[35] M. Izadi, H. Fagehi, A. Imanzadeh, S. Altnji, M.B.B. Hamida, M.A &Sheremet, Influence of finned charges on melting process performance in a thermal energy storage, Therm. Sci. Eng. Progress 37 (2023), 101547.

[36] M. Izadi, A. Hajjar, H.M. Alshehri, A. Saleem, A.M. Galal, Analysis of applying fin for charging process of phase change material inside H-shaped thermal storage, Int. Commun. Heat and Mass Transf. 139 (2022), 106421.

[37] M.M.S.M. Izadi, M.M. Shahmardan, M.J. Maghrebi, A &Behzadmehr, Numerical study of developed laminar mixed convection of Al2O3/water nanofluid in an annulus, Chem. Eng. Commun. 200 (7) (2013) 878–894.

[38] M. Izadi, M.M. Shahmardan, M. Norouzi, A.M. Rashidi, A &Behzadmehr, Cooling performance of a nanofluid flow in a heat sink microchannel with axial conduction effect, Appl. Phys. A 117 (2014) 1821–1833.

[39] H.B. Lanjwani, M.S. Chandio, M.I. Anwar, S.A. Shehzad, M &Izadi, Dual solutions of time-dependent magnetohydrodynamic stagnation point boundary layer micropolar nanofluid flow over shrinking/stretching surface, Appl. Math. Mech. 42 (7) (2021) 1013–1028.

[40] Q. Xiong, S. Altnji, T. Tayebi, M. Izadi, A. Hajjar, B. Sundén, L.K. Li, A comprehensive review on the application of hybrid nanofluids in solar energy collectors, Sustain. Energy Technol. Assessments 47 (2021), 101341.

[41] N. Neuberger, H. Adidharma, M. Fan, Graphene: a review of applications in the petroleum industry, J. Petroleum Sci. Eng. 167 (2018) 152–159.

[42] M. Shanbedi, S.Z. Heris, A. Amiri, E. Hosseinipour, H. Eshghi, S.N &Kazi, Synthesis of aspartic acid-treated multi-walled carbon nanotubes based water coolant and experimental investigation of thermal and hydrodynamic properties in a circular tube, Energy Conversion and Manag. 105 (2015) 1366–1376.

[43] D.K. Devendiran, V.A &Amirtham, A review of preparation, characterization, properties, and applications of nanofluids, Renew. Sustain. Energy Rev. 60 (2016) 21–40. A.

[44] E. Ebrahimnia-Bajestan, H. Niazmand, W. Duangthongsuk, S &Wongwises, Numerical investigation of effective parameters in convective heat transfer of nanofluids flowing under a laminar flow regime, Int. J. Heat Mass Transf. 54 (19–20) (2011) 4376–4388.

[45] R. Martínez-Cuenca, R. Mondragón, L. Hernández, C. Segarra, J.C. Jarque, T. Hibiki, J.E &Juliá, Forced-convective heat-transfer coefficient and pressure drop of water-based nanofluids in a horizontal pipe, Appl. Therm. Eng. 98 (2016) 841–849.

[46] K.A. Shah, B.A &Tali, Synthesis of carbon nanotubes by catalytic chemical vapor deposition: a review on carbon sources, catalysts, and substrates, Mater. Sci. Semicond. Process. 41 (2016) 67–82.

[47] P.N. Hong, D.N. Minh, N. Van Hung, P.N. Minh, P.H &Khoi, Carbon nanotube and graphene aerogels—The world's 3D lightest materials for environment applications: a review, Int. J. Mater. Sci. Appl. 6 (2017) 277.

[48] G.P. Sutton, O. Biblarz, Rocket Propulsion Elements, John Wiley and Sons Inc, New York, 2001.

[49] G. Leccese, E. Cavallini, M. Pizzarelli, State of art and current challenges of the paraffin-based hybrid rocket technology. AIAA Propulsion and Energy 2019 Forum, AIAA, Indianapolis, IN, 2019, p. 4010, https://doi.org/10.2514/6.2019-4010.

[50] G. Cheng, Y. Ito, D. Ross, Y.-.S. Chen, T.-.S. Wang, Numerical simulations of single flow element in a nuclear thermal thrust chamber, in: AIAA Paper 2007-4143, 39th AIAA Thermophysics Conference, 2007. Miami, FL.

[51] M. Mahmoodi, S &Kandelousi, The cooling process of the liquid propellant rocket by means of kerosene-alumina nanofluid, Propulsion and Power Res. 5 (4) (2016) 279–286.

[52] M. Mahmoodi, S.H &Kandelousi, Kerosene− alumina nanofluid flow and heat transfer for cooling application, J. Central South University 23 (2016) 983–990.

[53] M. Khan, M. Sarfraz, A. Ahmed, M.Y. Malik, A.S &Alqahtani, Study of engine-oil-based CNT nanofluid flow on a rotating cylinder with viscous dissipation, Physica Scripta 96 (7) (2021) 075005.

[54] M.I. Khan, S. Qayyum, F. Shah, R.N. Kumar, R.P. Gowda, B.C. Prasannakumara, S. Kadry, Marangoni convective flow of hybrid nanofluid (MnZnFe2O4-NiZnFe2O4-H2O) with Darcy Forchheimer medium, Ain Shams Eng. J. 12 (4) (2021) 3931–3938.

[55] U. Farooq, H. Waqas, M.S. Aldhabani, N. Fatima, A. Alhushaybari, M.R. Ali, T Muhammad, Modeling and computational framework of radiative hybrid nanofluid configured by a stretching surface subject to entropy generation: using Keller box scheme, Arabian J. Chem. (2023), 104628.

[56] N.S. Khashi'ie, N.M. Arifin, M. Sheremet, I. Pop, Shape factor effect of radiative Cu–Al2O3/H2O hybrid nanofluid flow towards an EMHD plate, Case Stud. Therm. Eng. 26 (2021), 101199.

[57] N. Acharya, K. Das, P.K &Kundu, On the heat transport mechanism and entropy generation in a nozzle of liquid rocket engine using ferrofluid: a computational framework, J. Computational Design and Eng. 6 (4) (2019) 739–750.